Lowland Technology International 2018; 19 (4): 245-250
International Association of Lowland Technology (IALT): ISSN 1344-9656
Special Issue on: Kumamoto Earthquake & Disaster

Research Paper

Analysis of liquefaction of volcanic soil during the 2016 Kumamoto Earthquake based on boring data

K. Ogo[1], H. Hazarika[2], T. Kokusho[3], D. Matsumoto[4], S. Ishibashi[5] and W. O. Sumartini[6]

ARTICLE INFORMATION

Article history:

Received: 06 March, 2017
Received in revised form: 15 February, 2018
Accepted: 18 February, 2018
Publish on: 09 March, 2018

Keywords:

Liquefaction
Boring data
Scanning electron microscope
Volcanic ash soil

ABSTRACT

On April 16th, 2016 Kumamoto earthquake registering 7 on Japanese scale caused liquefaction in many places around Kumamoto plain. However, considering the magnitude and the distance from the hypocenter, the liquefaction-induced damage was not so huge. Most of sand boiling was observed where liquefaction is likely to happen such as near waters and on an old river channel. In addition, black sand which seems to be volcanic soil was observed as ejecta of liquefaction in many places. This paper deals with the liquefaction characteristics of volcanic soil through physical and mechanical testing, microscopic observation by SEM and liquefaction susceptibility evaluation based on boring data. According to the physical testing, the grain size distribution was typical of liquefaction susceptible sand. Many of sand boils happened on the alluvial ground, and the thick strata of volcanic soil were found there. Based on the results of liquefaction evaluation, some locations have shown the liquefaction susceptibility in spite the fact that little occurrence of liquefaction took place at those locations.

1. Introduction

During the 2016 Kumamoto Earthquake, a foreshock of Mj 6.5 and a main shock of Mj 7.3 happened within 28 hours beneath Kumamoto City, Kumamoto Prefecture on Kyushu, Japan, both of which registered 7 on the Japanese seismic scale. The foreshock occurred on the Hinagu Fault at 21:26 JST on April 14, 2016, at an epicentral depth of about 11 kilometers. After some foreshocks, the main shock with a larger magnitude occurred on the Futagawa Fault at 01:25 JST on April 16, 2016 at an epicentral depth of about 10 kilometers. This was the strongest earthquake ever recorded in Kyushu since the Meteorological Agency of Japan (JMA) was established. More than 1,400 aftershocks have been recorded by JMA. A series of the earthquakes brought serious damage to cultural heritage and infrastructures such as roads, slopes and river embankments due to earthquake-induced landslides and debris flows, and fault-induced ground subsidence.

However, considering the magnitude and the distance from the hypocenter, the damage brought by liquefaction was not significant. Most of sand boils were observed where liquefaction is likely to happen such as near water places and an old river channel. One characteristic of the earthquake this time is that volcanic ash soil is observed as sand boiling at many palaces. (Hazarika et al., 2017) Various properties are expected to be different

[1] Kyushu University, Fukuoka 819-0395, JAPAN, katsuyasukt@gmail.com
[2] Professor , Kyushu University, Fukuoka 819-0395, JAPAN, hazarika@civil.kyushu-u.ac.jp
[3] Professor Emeritus, Chuo University, Tokyo 192-0395,JAPAN, koktak@ad.email.ne.jp
[4] Japan Foundation Engineering Co., Ltd. Osaka 530-0043, JAPAN, daisuke_matsumoto@jafec.co.jp
[5] Nihon Chiken Co., Ltd, Fukuoka 812-0894, JAPAN, ishibasi@chiken.co.jp
[6] Kyushu University, Fukuoka 819-0395, JAPAN, waode_sumartini@yahoo.co.id
Note: Discussion on this paper is open until September 2018.

for each volcanic ash soil (Egawa et al., 2016). The chemical component depends on the location of volcano and the time of eruption. The difference in the condition of sedimentation affects its mechanical characteristics. Moreover, aging effects might have reduced the damage from liquefaction, which strengthen the ground according to passage of time. Therefore, it is important to reveal the characteristics of volcanic soil in this region in order to explain the situation of the damage due to the earthquake from the geotechnical view.

This paper provides the results of physical and mechanical tests for the volcanic ash soil obtained during the reconnaissance survey covering major locations where damage was concentrated. The distribution of sand boils, boring data related to volcanic ash soil and ground water table and geological map are compared to understand the relationship between them. The study area is limited to the rectangular range, about 25 km from north to south, and 36 km from east to west, including south part of Nishi ku and Minami ku, Kumamoto city where liquefaction is likely to happen according to LiquickMap made by The National Institute of Advanced Industrial Science and Technology (2017).

2. Liquefaction-related damage in the Kumamoto Plain

Fig. 1 shows how sand boiling is distributed in the Kumamoto Plain. Sand boils are observed in some areas and the plots are crowded there. Comparing the aerial photos taken on April 15 and April 16, the size of the each sand boil deposit from the April 15 shots enlarged in the April 16 shots, which implies that the liquefied sites during the foreshock on April 14 were repeatedly liquefied druing the main shock of April 16 (Wakamatsu et al., 2017). Spots of liquefaction spreads along the Hinagu-Futagawa fault in 18 cities, towns and villages in Kumamoto prefecture. Most of those areas come under a geomorphological classification of natural levee, flood plain, old river channel and agricultural lands. The damage is especially significant along the Midorikawa river. In contrast, sand boils are seldom seen in the center of Kumamoto city.

Fig. 2 is a picture taken during the reconnaissance survey at a parking lot of JA (Japan Agricultural Cooperatives Group) office of Mashiki Town, where major building damage was observed due to the strong motion. Although many traditional Japanese style houses were damaged due to the strong motion, very few damage of liquefaction-induced settlement of national and prefectural roads and upliftment of manhole were observed.

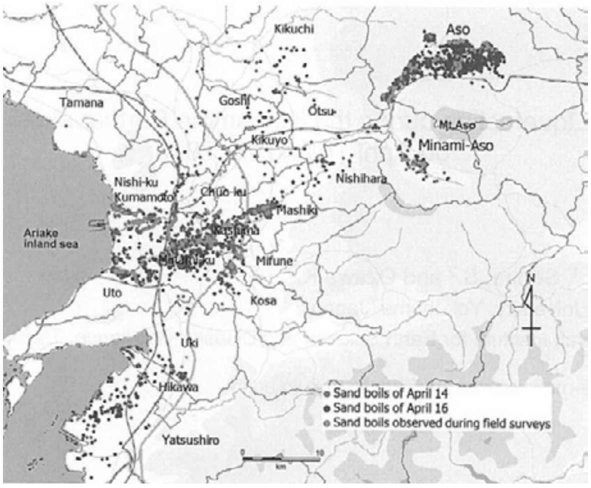

Fig. 1. Distribution of sand boiling in Kumamoto Plain (Wakamatsu et al., 2017)

Fig. 2. Sand boiling at a parking lot of JA-Kamimashiki

Fig. 3. Sand boiling in a house in Minami ku, Kumamoto

The Minami ward of Kumamoto city experienced liquefaction widely and intensively. Most of the damages were observed in the areas such as old river channel and floodplain. The Minami ward also includes the area developed by reclamation of an old river chanel, where intense liquefaction were observed. **Fig. 3** is damage due to ground subsidence observed in a residence in Minami ku, Kumamoto city. Sand boils were observed around this area and turned out to be black in color indicating volcanc soils.

Table 1 Sample list

No.	Location
1	Akita Higashi Primary School
2	Residence in Minami ku, Kumamoto -1
3	Residence in Minami ku, Kumamoto -2
4	Left Bank of the Shirakawa River
5	Akita Junior High School
6	JA Kamimashiki

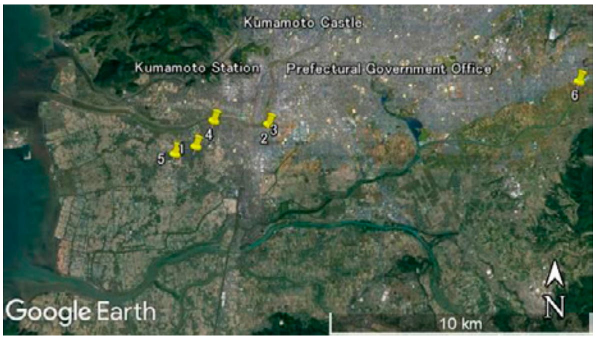

Fig. 4. Location of sampling

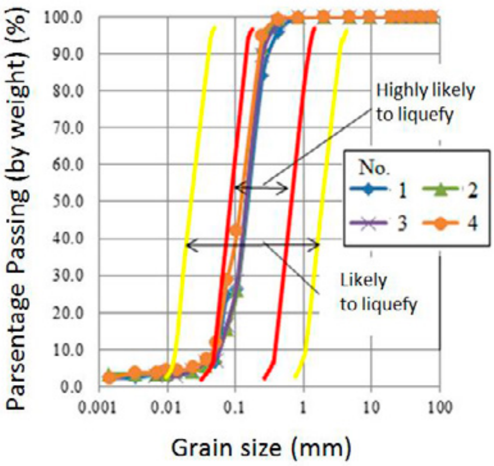

(a) U_C<3.5

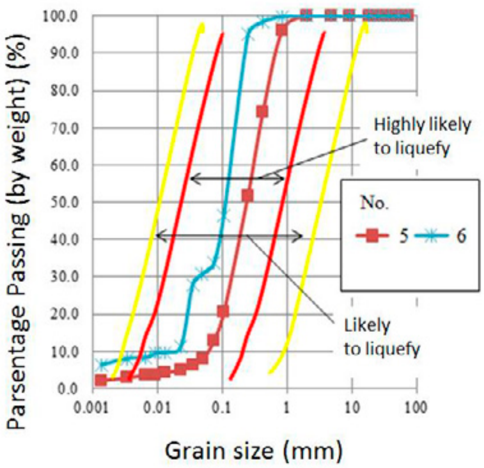

(b) $U_C \geqq 3.5$

Fig. 5. Grain size distribution and possibility of liquefaction

3. Physical testing of collected samples

Table 1 shows the list of collected samples in the site investigation after the Kumamoto Earthquake. Sample no. 1, 2, 3, 5 and 6 are taken from the sand boiling immediately after the earthquake, and no. 4 is sampled later from the nonliquefied riverbank to conduct a cyclic triaxial test. According to the result shown in **Fig. 5,** every distribution curve looks similar, and mainly consists of fine sand and medium sand. The results are compared with the criteria in Technical Standards and Commentaries for Port and Harbor Facilities in Japan. All the distributions are said to be highly likely to liquefy. According to Table 2, the particle density of ejecta is around 2.7 g/cm^3, which is relatively heavy in comparison with other sands. However, we also tested the maximum and minimum density of sample no. 5. The maximum dry density was 1.53 (g/cm^3) and the minimum dry density was 1.19, which was smaller than other soils.

Fig. 6 is the microphotograph of sample no. 2 observed with SEM. The shape of particle turned out to be angular. Hence, this microstructure could make more space among particles in the sedimentary structure, which makes the deposition density smaller despite the fact that its particle density is large.

Table 2 Particle density

No.	1	2	3	4	5	6
Density (g/cm^3)	2.761	2.697	2.655	2.631	2.758	2.598

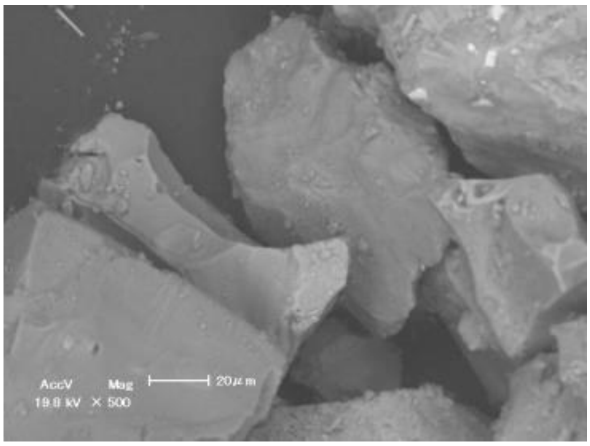

Fig. 6. Microphotograph of sample no. 6

4. Cyclic triaxial test

We conducted a cyclic triaxial test for sample no. 4 (JGS0541-2000). Water content is set at 30 %, and soil is compacted in a mold to make a specimen until its total

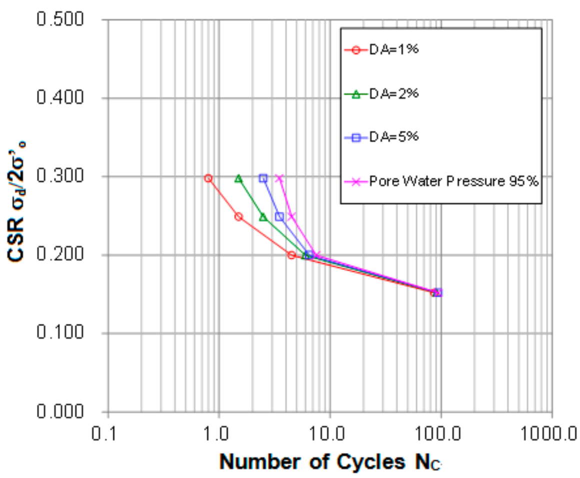

Fig. 7. Stress ratio-number of cycle relationship

density becomes 1.3 g/cm^3, according to the natural condition. The specimen dimension is 10 cm in height and 5 cm in diameter. 50 kPa of confining pressure is used during the consolidation and loading. According to **Fig. 7,** the value of CRR, cyclic resistance ratio at 20 cycles of loading, is 0.179. Generally, loose sand with the CRR less than 0.2 is likely to liquefy (Ishihara, 2017). Therefore, the specimen is vulnerable for liquefaction.

5. Effect of ground water table

In order to understand how ground water affected the distribution of liquefaction occurrence, the authors arranged the height of ground water table on the map in two ways: depth from the ground surface and the height of water surface in elevation. This value is based on the water levels in boreholes. If there are several data in one boring datum, the highest one is adopted.

5.1 The distribution of ground water table

Fig. 8 is the distribution of ground water level. The ground water table is high near the sea as expected.

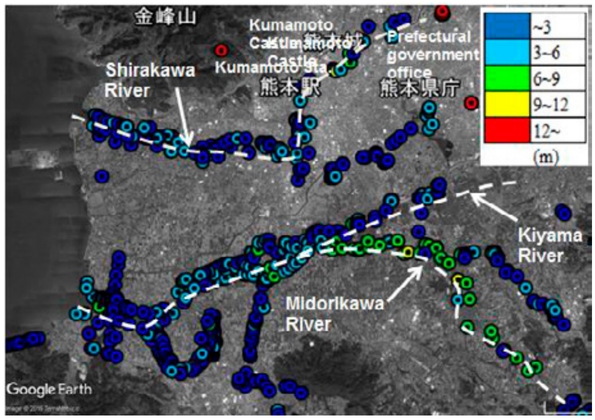

Fig. 8. Ground water table

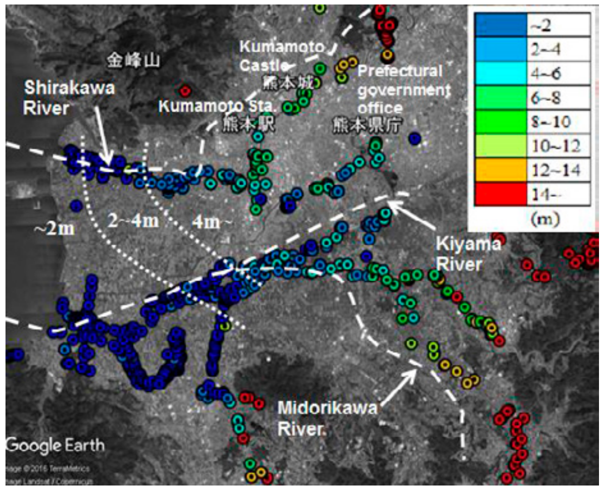

Fig. 9. Ground water level in elevation

However around the center of **Fig. 8** are many shallow spots (less than 6 m) , there are many deeper spots at the south side of those, though both areas are almost at the same distance from the sea. The north side is the central part of Kumamoto city, and the south side is where sand boiling occurred in many places. In **Fig. 9,** the numerical values stand for the height in elevation to see ground water levels in a unified standard. According to this figure, ground water table increases as the point

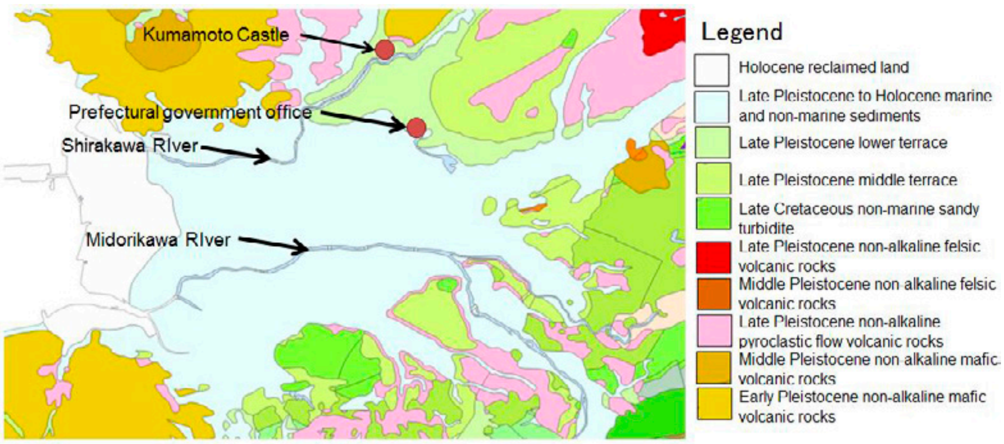

Fig. 10. Geologic map

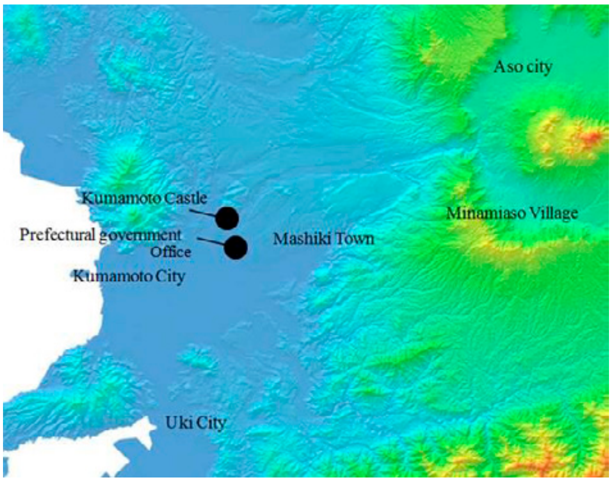

Fig. 11. Elevation map

gets far from the sea except the mountain areas.

5.2 Results and discussion

The difference of distribution between **Fig. 8** and **Fig. 9** is simply caused by the topographical height. Those data show that the possibility of liquefaction is dictated by the combination of the elevation, the distance from the sea and how the ground water table increases toward the inland areas. According to **Fig. 10,** most of sand boiling was seen on the new grounds. This explains the pattern of elevation shown in **Fig. 11.** New grounds are low, and that could result in high potential of liquefaction.

6. Distribution of volcanic ash soil

As a lot of ejecta were observed in many places which were made of volcanic ash soil, the authors need to establish some relationship between occurrence of liquefaction and the distribution of volcanic ash soil. It is assumed that there are two processes to form volcanic ash stratum: one is formed during the eruption, and the other is made of deposit transported by the river to form the lowlands. Once a volcanic eruption occurs, volcanic ash spreads and is piled up widely. Therefore, by knowing the distribution of volcanic ash soil, upper strata are presumed to be formed later.

Here, volcanic ash soil is declared to be volcanic ash soil in the borehole data, and we do not distinguish them by their process of deposit or the time of eruption. It shows the trend that the depth becomes larger near the sea and along the Midorikawa river. Locations with large depth correspond with the distribution of sand boiling. It can be said that grounds are relatively new where volcanic ash soil lies deep and it resulted in liquefaction. Because many borings data are from areas around rivers,

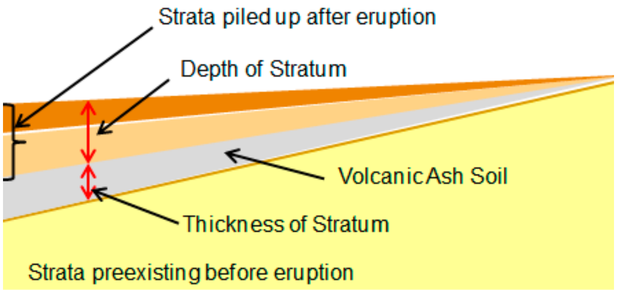

Fig. 12. Definition of depth and thickness of volcanic ash soil

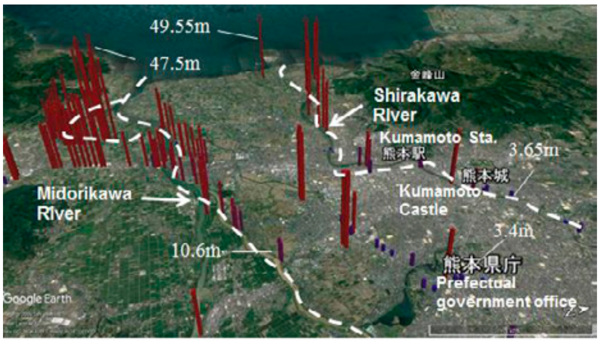

Fig. 13. Distribution of the depth of volcanic ash soil

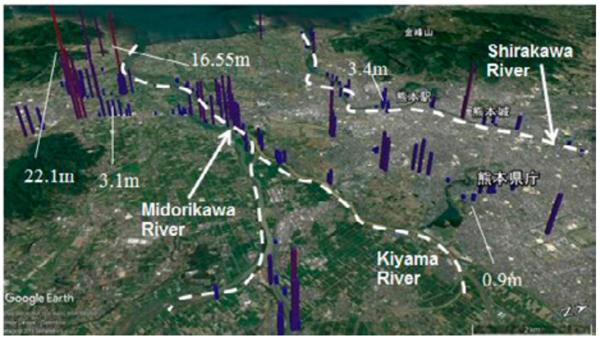

Fig. 14. Distribution of volcanic soil

the strata are affected by river conveying. However, at least, strata above the volcanic soil are presumed to be piled up later than the eruption. Concerning the fact that many sand boils are observed along the Midorikawa river, it can be assumed that this damage was caused due to the young formation of the ground there. Since the thickness of strata above the stratum of volcanic ash soil is deep, much sedimentation occurred after the formation of the volcanic stratum. It is understandable that much of a sand stratum above the volcanic ash soil were made of the transported material by the Midorikawa river, which conveys sand and gravels. As a result, the sand stratum was vulnerable enough to liquefy. Therefore, the depth of volcanic stratum does not mean that of liquefied layer but just indicates how much new ground is above the volcanic stratum in comparison. **Fig. 14** is also the distribution of volcanic ash soil, and the graph means the thickness of the stratum of volcanic ash soil. The amount of sedimentation is higher along the Midorikawa river. Considering the mechanism of sedimentation, spots with large numerical value were likely to be under the water when volcanic eruption occurred.

7. Conclusions

Based on the information from the boring data and the geologic map, the following conclusions could be drawn.

1) Regarding the characteristics of the volcanic ash soil, its density was large in comparison with other soils, and it consists mainly of fine sand and medium sand. It also showed little resistance to liquefaction in cyclic triaxial test.

2) Most of sand boils were observed on the alluvial plain;

3) There were no significant difference in ground water table between liquefied sites and unliquefied sites.

4) When this ground water table is organized according to the elevation on the map, it rose up toward the center of Kumamoto City, where little liquefaction was observed. The difference of the sedimentary structure might affect the direction of ground water. In order to understand how the volcanic ash soil is affected by the geology and passage of time, further research is required about its physical and mechanical property.

Acknowledgements

The financial grant for this research under the J-RAPID program (Principal Investigator: Hemanta Hazarika) of Japan Science and Technology Agency (JST) is gratefully acknowledged.

References

Hazarika, H., Kokusho, T., Kayen, R. E., Dashti, S., Fukuoka, H., Yasuhara, K., Saitoh, O., Sakai, N., Ishizawa, T. and Chen, G., 2016. An overview of the geotechnical damage brought by the 2016 Kumamoto Earthquake. International Society for Soil Mechanics and Geotechnical Engineering (ISSMGE) Bulletin, **10** (3).

Hazarika, H., Kokusho, T., Kayen, R. E., Dashti, S., Fukuoka, H., Ishizawa, T., Kochi, Y., Matsumoto, D., Hirose, T., Furuichi, H., Fujishiro, T., Okamoto, K., Tajiri, M. and Fukuda, M., 2018. Geotechnical damage due to the 2016 Kumamoto Earthquake and future challenges. Lowland Technology International, **19** (3): 189-204.

Kayen, R., Dashti, S., Kokusho, T., Hazarika, H., Franke, K., Oettle, N., Wham, B., Calderon, J.R., Briggs, D., Guillies, S., Cheng, K., Tanoue, Y., Takematsu, K., Matsumoto, D., Morinaga, T., Furuichi, H., Kitano, Y., Tajiri, M., Chaudhary, B., Nishimura, K. and Chu, C., 2016. Geotechnical aspects of the 2016 MW6.2, MW 6.0, and MW 7.0 Kumamoto Earthquakes. University of Berkeley, GEER Report.

Wakamatsu, K., Senna, S. and Ozawa K., 2017. Liquefaction during the Kumamoto Earthquakes on April 14 and 16, 2016, Proc. of the International Workshop on the 2016 Kumamoto Earthquake. March 6, 2017, Kyushu Univ., Fukuoka, Japan: 123-128.

Kiyota T., 2017. The mechanism of liquefaction and the characteristics of its damage. http://yumenavi.info/lecture.aspx?GNKCD=g005255, 2017. (In Japanese).

Egawa T., Yamanashi, T. and Tomisawa K., 2016. Study on Liquefaction Characteristics of Volcanic ash soil – Report on Field Investigations in Hokkaido-. Journal of JAEE (Japan Association for Earthquake Engineering) **16** (1): 352-364.

Murakami S. and Nagase H., 2016. Liquefaction damage in The 2016 Kumamoto Earthquake. Japanese Geotechnical Society the 2016 Kumamoto Earthquake Geodisaster Report. https://www.jiban.or.jp/images/saigai/H28Kumamoto_jisinsaigai_0511ekijoka.pdf, 2017 (In Japanese).

Geospatial Information Authority of Japan, 2017. Basic map information download service. Numerical elevation model, http://fgd.gsi.go.jp/download/menu.php (In Japanese).

The National Institute of Advanced Industrial Science and Technology, 2017. Seamless geographic map. https://gbank.gsj.jp/seamless/, 2017 (In Japanese).

AIST, 2017. LiquickMap. https://gbank.gsj.jp/QuiQuake/LiquickMap/, 2017 (In Japanese).

Ministry of Land, Infrastructure, Transport and Tourism, 2017. KuniJiban. http://www.kunijiban.pwri.go.jp/jp/GSImap/GSImap.html, 2017 (In Japanese).

Ishihara K., 2017. Liquefaction of ground. Asakura Publishing Co., Ltd., 6-29 Shin-ogawa Machi, Shinjuku ku, Tokyo, Japan: pp. 108 (In Japanese).

Symbols and abbreviations

N_c	Number of Cycles
CRR	Cyclic Resistance Ratio
CSR	Cyclic Stress Ratio